

# Laser kinetic spectroscopy of the interfacial charge transfer between membrane cell walls of *E. coli* and TiO<sub>2</sub>

V. Nadtochenko<sup>a,\*</sup>, N. Denisov<sup>a</sup>, O. Sarkisov<sup>b</sup>, D. Gumy<sup>c</sup>, C. Pulgarin<sup>c</sup>, J. Kiwi<sup>d,\*\*</sup>

<sup>a</sup> Institute of Problems in Chemical Physics, Russian Academy of Sciences, 142432 Chernogolovka Moscow Region, Russia

<sup>b</sup> Institute of Chemical Physics, Russian Academy of Sciences, 101999 Moscow, Russia

<sup>c</sup> Institute of Chemical Sciences and Engineering, Group of Electrochemical Engineering, Station 6, Switzerland

<sup>d</sup> Laboratory of Photonics and Interfaces, Swiss Federal Institute of Technology, EPFL-SB-LPI, 1015 Lausanne, Switzerland

Received 23 September 2005; received in revised form 13 December 2005; accepted 27 December 2005

Available online 28 February 2006

## Abstract

This laser kinetics features of the electron decay of TiO<sub>2</sub> in the presence of the *Escherichia coli* (*E. coli*) phosphatidyl-ethanolcholine (PE) and lipo-polysaccharides (LPS) cell wall components were reported in this study. The interaction of the biomolecules with the photogenerated charge carriers was determined and the reaction rates were measured. The effect of the variation of ionic strength of the colloidal TiO<sub>2</sub> on the electron decay was determined in the presence of PE and *E. coli*. The ionic strength seems to affect the equilibrium absorption of the biomolecules on TiO<sub>2</sub>. The e<sup>-</sup> decay was measured for TiO<sub>2</sub> samples having different sizes, charge and isoelectric points (IEP) by laser spectroscopy for different types of TiO<sub>2</sub>. TiO<sub>2</sub> Degussa P-25 mediated the *E. coli* abatement most effectively compares to other TiO<sub>2</sub> samples. The structural features of different TiO<sub>2</sub> samples were related to the degradation of *E. coli* and also related to the fast kinetics results.

© 2005 Elsevier B.V. All rights reserved.

**Keywords:** Photocatalysis; TiO<sub>2</sub>; *E. coli*; Bacteria; Interface

## 1. Introduction

The use of TiO<sub>2</sub> as a photocatalyst with bactericide properties has become a field of increasing interest after the pioneering work of Hashimoto and Fujishima [1–3], Blake [4,5], and Egerton [6]. The bactericidal properties of TiO<sub>2</sub> were recognized around 1985 [7–10] and were attributed to the high redox potential of the surface species formed by photo-oxidation, affording non-selective oxidation of bacteria. More recently, our laboratory has carried out work of TiO<sub>2</sub> mediated photocatalytic peroxidation of *Escherichia coli* membrane cell [11–14]. Photocatalytic damage of the cell wall is due to the interfacial transfer of charge carriers of highly oxidative radicals on the TiO<sub>2</sub> surface after the laser pulse. The formation of oxidative surface radical-species on TiO<sub>2</sub> has been shown to depend on particle size, crystalline phase, BET area and the structure of the TiO<sub>2</sub> aggregate [15] in aqueous media. The effect of the type of TiO<sub>2</sub>

on the *E. coli* photokilling has been reported recently [16–19] using *E. coli* K12. This strand has been selected since it is readily accessible in a pure form and presents a uniform size of 1 μm.

The quantum efficiency of radicals generation at the TiO<sub>2</sub> surface is determined by the competition of the interfacial charge carriers transfer with the molecules in contact with the TiO<sub>2</sub> surface and the kinetics of e<sup>-</sup>, h<sup>+</sup> charge recombination. These processes are complicated by the fact that several light activated processes take place simultaneously during the TiO<sub>2</sub> photocatalytic abatement of bacteria. Very few studies report on the fast kinetics of the electrons and holes reactions in their competition between charge recombination and/or their transfer to biomolecules or bacteria in contact with TiO<sub>2</sub> [20,21].

This study addresses the interfacial charge transfer between TiO<sub>2</sub> nanoparticles and the cell wall membrane components and *E. coli* itself. It is our aim to determine how the TiO<sub>2</sub> photogenerated charge carriers react with the *E. coli* cell wall membranes like phosphatidyl-ethanolcholine (PE) and lipo-polysaccharides (LPS): does the interfacial charge transfer process occur between photoexcited TiO<sub>2</sub> and the *E. coli* wall, PE, or LPS? PE is the major phospholipid component of *E. coli* constituting ~70–80%

\* Corresponding author. Tel.: +7 096 522 40 21.

\*\* Corresponding author.

E-mail address: [nadto@icp.ac.ru](mailto:nadto@icp.ac.ru) (V. Nadtochenko).

of the total amount of phospholipid present. Lipopolysaccharide (LPS) is positioned in the outer monolayer of the non-symmetrical outer bilayer in *E. coli*. The photocatalytic activity during the abatement of *E. coli* for some selected TiO<sub>2</sub> colloids is measured and then correlated with the amount of photogenerated charges that survive recombination within the picosecond to microsecond time range.

## 2. Experimental

### 2.1. Materials

TiO<sub>2</sub> Degussa P-25 (50 m<sup>2</sup>/g), TiO<sub>2</sub> Tayca TKS-203 (~240 m<sup>2</sup>/g) and TiO<sub>2</sub> S5-A300 (280 m<sup>2</sup>/g) and S5-B300 (250 m<sup>2</sup>/g) were obtained from Degussa AG, Millennium Inorganic Chemicals and Tayca Corp., respectively. The addresses of the suppliers are stated below in the acknowledgment. The TiO<sub>2</sub> samples used were selected for their efficient bacterial abatement under solar irradiation and their transient absorption characteristics in the presence of cell wall membranes and *E. coli*. The LPS from *E. coli* Serotype O55:B5 (code 446248/1 41303086) was Fluka AG, Biochemica and used as received. L- $\alpha$ -phosphatidylethanolamine (L- $\alpha$ -cephaline) from bovine brain was also Fluka AG and was used without further purification. For bacterial tests, *E. coli* K12 DSM ATCC 23716 was obtained from DZMZ GmbH Germany, cat. no. 23716.

### 2.2. Irradiation procedures

Samples were illuminated in the temperature controlled cavity Suntest solar light simulator from the Heraeus AG (Hanau, Germany) with a spectral distribution with 7% of the photons between 300 and 400 nm. The photons in the visible region of the spectrum range up to 800 nm and followed the intensity profile of the spectral distribution of the solar spectrum. The radiant flux was monitored with a Kipp & Zonen (CM3) power meter. The irradiation of samples containing *E. coli* was carried out in the closed aluminium box cavity of the Suntest simulator. The reflection coefficient of the wall was close to 93%. The light power density reaching the samples was observed to depend only marginally on the position of the sample in the box.

### 2.3. Photochemical experiments leading to the abatement of *E. coli* K12

A Pyrex glass of 50 ml (3 cm in diameter and 5 cm high) was used as a cylindrical batch photoreactor for the *E. coli* K12 lyophilized bacterial strands. Experiments were carried out in saline solution (8 g/l NaCl and 0.2 g/l KCl in Milli-Q water). A TiO<sub>2</sub> concentration of 0.2 g/l was used during the experiments. The solutions were stirred in the photoreactor during the runs. The results of the *E. coli* abatement (CFU/ml) at pre-selected photocatalysis times were the average of three experimental points.

### 2.4. Laser photolysis

The nanosecond laser photolysis study used the third harmonic of the Nd<sup>3+</sup>:YAG, 354 nm, 10 ns laser pulse. The suspension of TiO<sub>2</sub> with and without addition of *E. coli*, LPS or PE in the form of SUV was investigated in a 1 mm cell in contact with air at 20 °C. For the solutions requiring high optical transparency, the supernatant fraction after sedimentation for 20 days of TiO<sub>2</sub> Degussa P-25 was used and when other TiO<sub>2</sub> samples were used, the finest fraction after a long sedimentation period was used due to the optical penetration required during the laser experiments. Femtosecond laser photolysis was carried out by pump-probe technique with using of white super-continuum as a probe pulse (400–900 nm). TiO<sub>2</sub> was excited by  $\lambda = 308$  nm pump pulse with duration of 70 fs [22].

### 2.5. Bacterial strain and growth medium

The bacterial strain used *Escherichia coli* (*E. coli* K12) was inoculated in to nutrient broth (Oxoid no. 2, Switzerland) and grown overnight at 37 °C. During the stationary growth phase, bacteria cells were harvested by centrifugation at 500G for 10 min at 4 °C. The bacterial pellet was then washed three times with the saline solution. Cell suspensions were inoculated in the saline solution in the Pyrex glass bottle of 50 ml to a cell density of 10<sup>6</sup>–10<sup>7</sup> colony forming units per milliliter (CFU/ml). Serial dilutions were prepared if necessary in the saline solution and 100  $\mu$ l samples were plated on Plate-Count-Agar (PCA, Merck, Germany). Plates were incubated at 37 °C for 48 h before the bacterial counting was carried out.

### 2.6. Zeta potential and attenuation aggregate size

A Colloidal Dynamics AcoustoSizer II (Sydney, Australia) instrument has been used during this work [23]. The electroacoustic procedure measures the *dynamic mobility*, which is the frequency analogue of the direct current (dc) mobility. These acoustic methods can be applied to dilute [23] and concentrated aqueous suspensions [24]. O'Brien derived the formula that allows a link between *dynamic mobility* to particle size and zeta potential [25] assuming that the zeta potential is independent of the particle size and shape, but approximates the particle geometry to spherical particles. The suspensions were prepared by dispersing 3–4 g of powder in 150 ml KNO<sub>3</sub> (0.01 M) (2.5 wt.% powder) and the pH adjusted with HNO<sub>3</sub> to around 3 and then titrated up to pH 10 or 11 by addition of KOH (0.01 M) 25 °C. The zeta potential is calculated using Smoluchowski's equation [26] for thin double layers ( $\kappa_a > 20$ ). The double layer of 10 nm expected for the ionic background concentration used of 0.01 M is much smaller than the size of the aggregate particles.

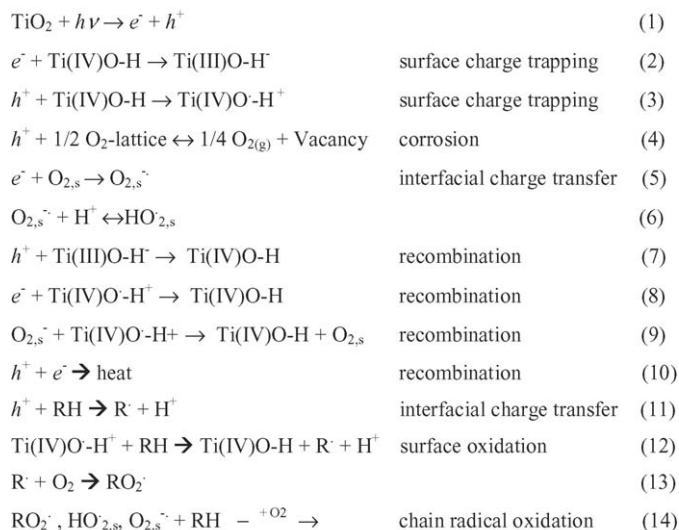
## 3. Results and discussion

### 3.1. Charge recombination in TiO<sub>2</sub> Degussa P-25 in the absence and presence of PE, LPS and *E. coli*

The relevant feature of the laser photolysis experiments is that the addition of the biomolecules *E. coli*, PE or LPS to a

TiO<sub>2</sub> colloid modifies the transient decay of photoexcited TiO<sub>2</sub> (Degussa P-25). Control experiments showed no signals for the transient absorption due to *E. coli*, PE or LPS suspensions by themselves. The effect of biomolecules on the transient decay in TiO<sub>2</sub> was observed only in the nanosecond and millisecond time scale. In the femtosecond–picosecond time scale (100 fs–40 ps) the effect of LPS or PE addition on the transient decay was negligible.

The spectra and transient decay of photoexcited TiO<sub>2</sub> has been recently reported [15]. It was shown that the transient absorbance in the visible  $\lambda > 600$  nm is determined by the absorbance of the electron from the conduction band and/or by TiO<sub>2</sub> trapped electrons [13,15,22]. The effect of the *E. coli*, PE and LPS addition on transients of TiO<sub>2</sub> is shown in Fig. 1. Fig. 1(a) shows the effect of *E. coli* on the e<sup>-</sup> decay. A similar effect was observed upon addition of PE or LPS to colloidal TiO<sub>2</sub> and is reported in Fig. 1(b) and (c) on the e<sup>-</sup> decay. By inspection of Fig. 1(a)–(c), it is seen that the e<sup>-</sup> decay in TiO<sub>2</sub> becomes slower after addition of *E. coli*, PE or LPS. Scheme 1, in agreement with widely accepted evidence available in this field, presents the main events involving the fate of the e<sup>-</sup> and h<sup>+</sup> charge carriers in TiO<sub>2</sub>. Fig. 1 shows that h<sup>+</sup> in Scheme 1, is scavenged by *E. coli*, PE or LPS (reactions 11, 12). It leads to the increase of the e<sup>-</sup> life-time, because e<sup>-</sup>/h<sup>+</sup> recombination processes 8, 10 are in the competition with reaction of 11 and 12. The results reported in Fig. 1 provide the evidence the interfacial charge transfer between photoexcited TiO<sub>2</sub> and organic biomolecules like *E. coli*, PE or LPS.



O<sub>2,s</sub>, O<sub>2,s</sub><sup>-</sup>, HO<sub>2,s</sub> adsorbed at TiO<sub>2</sub> surface  
O<sub>2(g)</sub> gaseous oxygen

Scheme 1.

Transient kinetics shows the complex non-exponential decay in Fig. 1. This complicates the quantitative analysis of the biomolecules effect on the transient decay. The mean lifetime of the transients can be estimated from the expression  $\langle \tau \rangle = \int P(t) dt$ , where  $P(t)$  is the survival probability of the

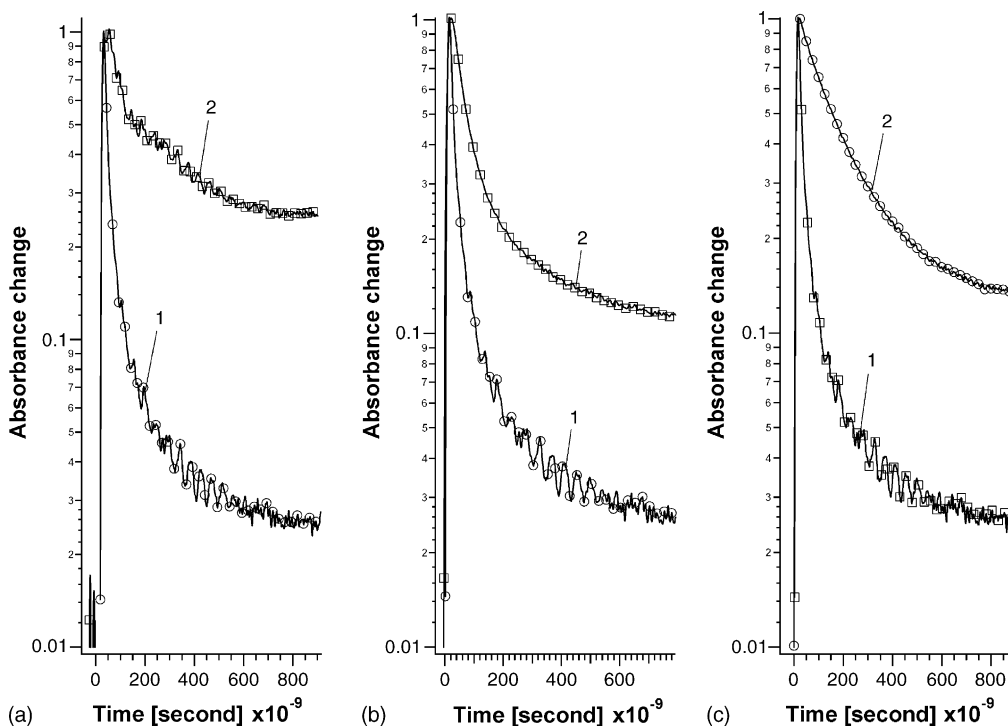


Fig. 1. (a) Effect of *E. coli* on the e<sup>-</sup> decay registered at  $\lambda = 820$  nm obtained from nanosecond laser photolysis. Laser pulse  $\lambda = 354$  nm. Trace (1) decanted colloidal solution of TiO<sub>2</sub> Degussa P-25 and trace (2) decanted colloid of TiO<sub>2</sub> Degussa P-25 trace in the presence of  $3 \times 10^7$  CFU/ml *E. coli*. (b) Nanosecond decay of a colloid of TiO<sub>2</sub> Degussa P-25 in the absence and in the presence of phosphatidyl-ethanolcholine (PE). Trace (1) decanted colloid of TiO<sub>2</sub> Degussa P-25 and trace (2) decanted colloid of TiO<sub>2</sub> Degussa P-25 in the presence of 12 mg/ml PE. (c) Nanosecond decay laser pulse decay of a colloid of TiO<sub>2</sub> Degussa P-25 in the absence and in the presence of the lipo-polysaccharide (LPS). Trace (1) shows decanted colloid of TiO<sub>2</sub> Degussa P-25 and trace (2) shows decanted colloid of TiO<sub>2</sub> Degussa P-25 trace in the presence of 1 mg/ml LPS.

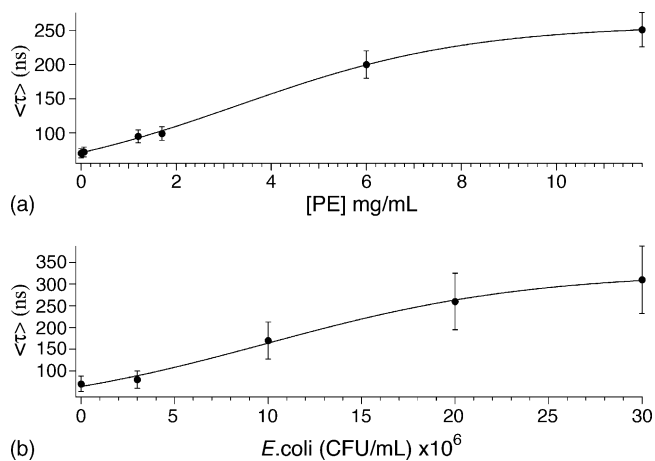


Fig. 2. The dependence of the mean life-time  $\langle \tau \rangle$  of  $e^-$  decay on: (a) the concentration of PE; (b) the concentration of *E. coli*.  $TiO_2$  is decanted colloid of  $TiO_2$  Degussa P-25.

transient. The reciprocal value of  $\langle \tau \rangle$  can be considered as the mean rate constant of the decay process. The ratio of  $\tau$  values estimated from Fig. 1 for the  $e^-$  transient decay in the presence and in the absence of the biomolecules were:  $\langle \tau_{P25TiO_2} \rangle = 70$  ns;  $\langle \tau_{P25TiO_2 E. coli} \rangle = 310$  ns;  $\langle \tau_{P25TiO_2 LPS} \rangle = 160$  ns;  $\langle \tau_{P25TiO_2 PE} \rangle = 252$  ns. There is a meaningful increase of the life-time of  $e^-$  in Degussa P-25  $TiO_2$  as a result of the  $h^+$  scavenging by biomacromolecules.

The effect of biomolecules concentration on  $e^-$  decay in  $TiO_2$  was tested with PE vesicles as a probe. The effect of PE vesicles on the electron decay is a function of the concentration of PE. The mean life-time  $\langle \tau \rangle$  of  $e^-$  decay in  $TiO_2$  increased with the increase of PE concentration in the range of 0–11.8 mg/ml as shown in Fig. 2a. The increase of *E. coli* concentration also

leads to the increase of the  $\langle \tau \rangle$  value (Fig. 2b). In both cases this dependency of  $\langle \tau \rangle$  shows a saturation-like curve. The observed dependence suggest that  $h^+$  holes are scavenged by PE or *E. coli* organic material. In the limit of high concentrations of PE and *E. coli* the mean life-times were comparable with the values  $\langle \tau_{P25TiO_2 PE} \rangle = 252 \pm 25$  ns;  $\langle \tau_{P25TiO_2 LPS} \rangle = 310 \pm 77$  ns. A comparable ability of PE and *E. coli* cells to scavenge  $h^+$  in  $TiO_2$  nanoparticles may account for the results observed. Unfortunately, the complex form of  $e^-$  decay profiles prevents the exact estimation of the probability to scavenge the hole by PE or *E. coli* at the high concentration limit. If holes are not completely scavenged by organic probes added to  $TiO_2$  then the  $e^-$  decay is determined by reactions 2 and 5 and probably by the recombination with residual holes in reactions 8 and 10. The ratio of mean rate constants of  $e^-$  decay at zero concentration of organic material and at the high concentration is close to 3.6 for PE and 4.4 for *E. coli*.

### 3.2. Ionic strength effects on the kinetics of charge transfer between $TiO_2$ Degussa P-25 and PE or *E. coli*

Figs. 3–5 show the effect of the NaCl and  $CaCl_2$  on the  $TiO_2$   $e^-$  decay for solutions containing PE and *E. coli*. Fig. 3 shows the NaCl effect on the charge transfer between  $TiO_2$  Degussa P-25 in the presence of PE. The addition of 6 mg/ml of PE increases the  $\langle \tau_{P25TiO_2} \rangle = 70$  ns up to  $\langle \tau_{P25TiO_2 PE} \rangle = 195$  ns. About 1 M NaCl decreases the  $\langle \tau_{P25TiO_2 PE} \rangle = 195$  ns down to 84 ns. In the control experiment, the addition of 1 M NaCl to the net  $TiO_2$  Degussa P-25 does not lead to meaningful changes of the transient curve of  $e^-$  decay in the present experiment. The additional argument that  $Cl^-$  is not important in the particular case as a possible hole scavenger is the NaCl effect was in the opposite way that could be expected if  $Cl^-$  participates as a  $h^+$  scavenger.

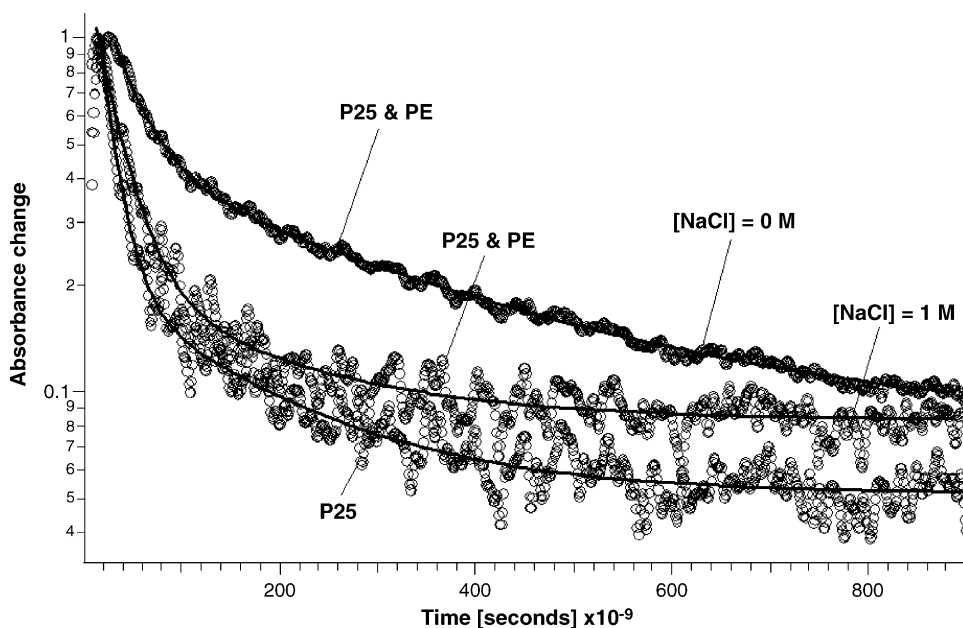


Fig. 3. Effect of NaCl on the  $e^-$  decay in a colloid of  $TiO_2$  Degussa P-25 in the presence of the bilayer vesicles of PE. PE concentration is 6 mg/ml. Traces are labeled as: P-25 is net  $TiO_2$  colloid; P-25 and PE with  $[NaCl] = 0$  M is the same concentration of  $TiO_2$  P-25 with addition of 6 mg/ml of PE vesicles; P-25 and PE with  $[NaCl] = 1$  M is the same concentration of  $TiO_2$  P-25 with addition of 6 mg/ml of PE vesicles.

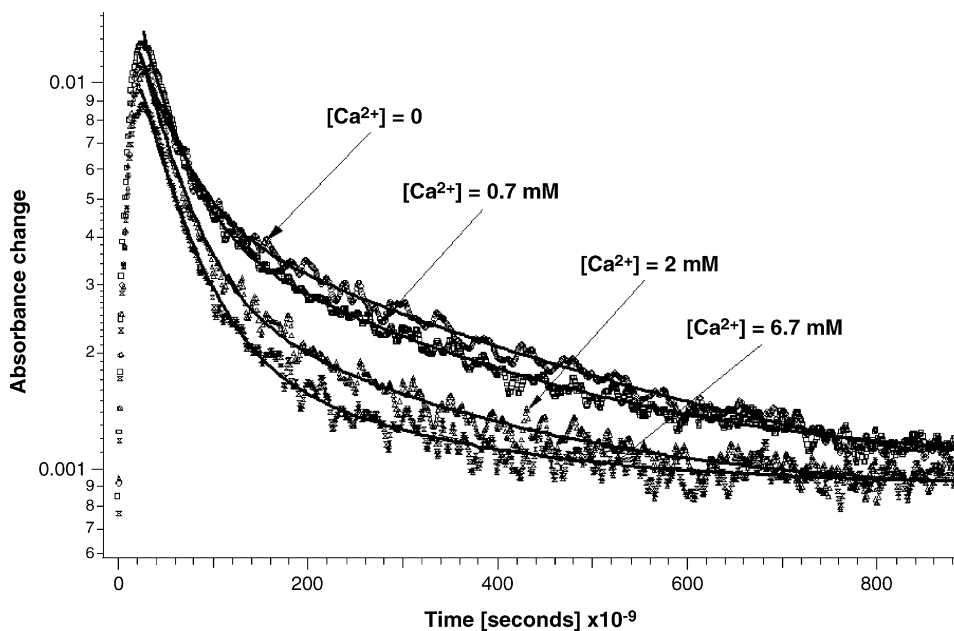


Fig. 4. Effect of  $\text{CaCl}_2$  on the  $e^-$  decay in a colloid of  $\text{TiO}_2$  Degussa P-25 in the absence and in the presence of the bilayer vesicles PE.  $[\text{CaCl}_2]=0\text{ M}$ ,  $\langle\tau\rangle=196\text{ ns}$ ;  $[\text{CaCl}_2]=0.7\text{ mM}$ ,  $\langle\tau\rangle=166\text{ ns}$ ;  $[\text{CaCl}_2]=2\text{ mM}$ ,  $\langle\tau\rangle=154\text{ ns}$ ;  $[\text{CaCl}_2]=6.7\text{ mM}$ ,  $\langle\tau\rangle=140\text{ ns}$ .

Fig. 4 shows the effect of the concentration of the  $\text{CaCl}_2$  salt added on the  $e^-$  decay in colloidal solutions of  $\text{TiO}_2$  Degussa P-25 in the presence of PE. A specific feature of  $\text{CaCl}_2$  is the effect on  $e^-$  decay at very low concentration of  $\text{CaCl}_2$  in the millimole range. The addition of  $\text{Ca}^{2+}$  in Fig. 4 is seen to be effective in increasing the  $e^-$  decay at a much lower concentration than  $\text{NaCl}$  in Fig. 3. These two salts increase the  $e^-$  decay rate. From Fig. 4 it is seen that the addition of  $\text{CaCl}_2$  at concentrations above 2 mM leads to a saturation effect:  $\langle\tau\rangle=154\text{ ns}$  when  $[\text{CaCl}_2]=2\text{ mM}$  and  $\langle\tau\rangle=150\text{ ns}$  when  $[\text{CaCl}_2]=6.7\text{ mM}$ .

Fig. 5 reports the experimental results found for  $\text{TiO}_2$  Degussa P-25 colloids in the absence and presence of *E. coli*

and after addition of  $\text{NaCl}$  1 M ( $\langle\tau\rangle=390\text{ ns}$ ) and  $\text{NaCl}$  2M ( $\langle\tau\rangle=420\text{ ns}$ ). It is readily seen in Fig. 5 that the  $e^-$  decay rate is decreased when the concentration of  $\text{NaCl}$  was increased.  $\text{NaCl}$  acts in the opposite way for the *E. coli* system as it was in the case of PE. The addition of  $\text{Ca}^{2+}$  to a colloid of Degussa P-25  $\text{TiO}_2$  is not possible in the presence of *E. coli* since the colloid precipitated. The transparency of the solution was lost in the  $\text{TiO}_2/\text{LPS}$  system when salt was added. The transparency necessary for optical experiments was not more available.

The observed salt effect has a complex nature. It can be rationalized in terms of the adsorption/contact of biomolecule on the  $\text{TiO}_2$  surface. The decrease of  $e^-$  decay for *E. coli* system

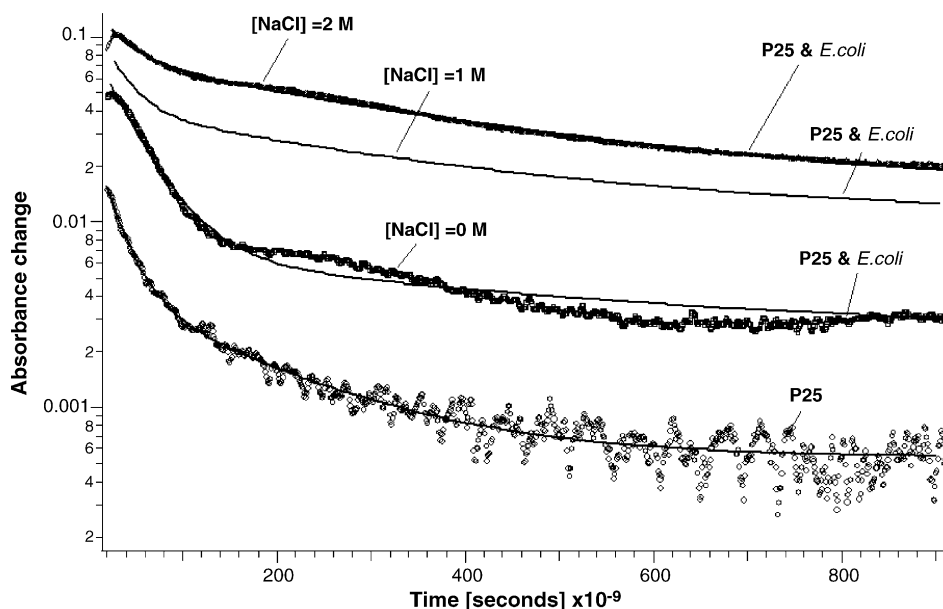


Fig. 5. Effect of  $\text{NaCl}$  on the  $e^-$  decay in a colloid of  $\text{TiO}_2$  Degussa P-25 in the absence and in the presence of *E. coli*.

Table 1  
Abatement of *E. coli* by TiO<sub>2</sub> samples with irradiated with Suntest solar simulator during 4 h (65 mW/cm<sup>2</sup>) at pH 6

Type of TiO <sub>2</sub>	Abatement (CFU/ml)	Crystalline phase	BET (m <sup>2</sup> /g)	Median particle <sup>a</sup> size (nm)	Attenuation aggregate size (nm)	IEP
Degussa P-25	10 <sup>7-8</sup> × 10 <sup>1</sup>	Anat-rutile	56	25–35	370	7.0
Millennium S5-300A	10 <sup>7-2</sup> × 10 <sup>2</sup>	Anatase	280	30–60	1500	7.0
Millennium S5-300B	10 <sup>7-1</sup> × 10 <sup>3</sup>	Anatase	250	30–60	1300	4.9
Tayca TKS203	10 <sup>7-3</sup> × 10 <sup>3</sup>	Anatase	241	6	200	<3

<sup>a</sup> The median particle size  $d_n$  was determined by TEM of a few hundred particles [28].

with NaCl addition can be considered as an indication that the increase in NaCl concentration favours the binding between *E. coli* and TiO<sub>2</sub> Degussa P-25. The NaCl is known to regulate the contact between PE vesicles and TiO<sub>2</sub>. Therefore, the increase of  $e^-$  decay for PE with NaCl addition lead to a decrease of the binding between TiO<sub>2</sub> and PE. Ca<sup>2+</sup> concentration is an important agent controlling the bilayer potential in biological systems. [10,20]. A small amount of Ca<sup>2+</sup> affects the  $e^-$  decay in the PE system, and at the same time provokes the precipitation in the TiO<sub>2</sub> colloid with *E. coli*.

### 3.3. Charge recombination of different TiO<sub>2</sub> samples and their relation to the inactivation of *E. coli* under continuous solar irradiation at pH 6

Fig. 6 shows the inactivation of *E. coli* within the first hour of reaction with different photocatalysts like: TiO<sub>2</sub> Degussa P-25, TiO<sub>2</sub> S5-A300, S5-B300 and TiO<sub>2</sub> TKS 203 anatase. Under steady state illumination, the TiO<sub>2</sub> Degussa P-25 was the most efficient photocatalyst. To further explore this point, Table 1

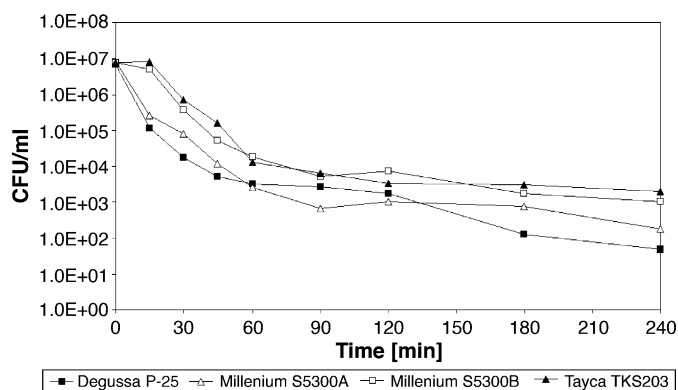


Fig. 6. *E. coli* survival using different TiO<sub>2</sub> samples irradiated with a Suntest solar simulator during 4 h with a dose of 65 mW/cm<sup>2</sup> at pH 6.

shows the properties of TiO<sub>2</sub> S5-A300, TiO<sub>2</sub> S5-B300 and TiO<sub>2</sub> TKS 203. The later catalysts show a considerable bigger surface area, a different crystallography and attenuated aggregate size with respect to TiO<sub>2</sub> Degussa P-25. But the last one is faster

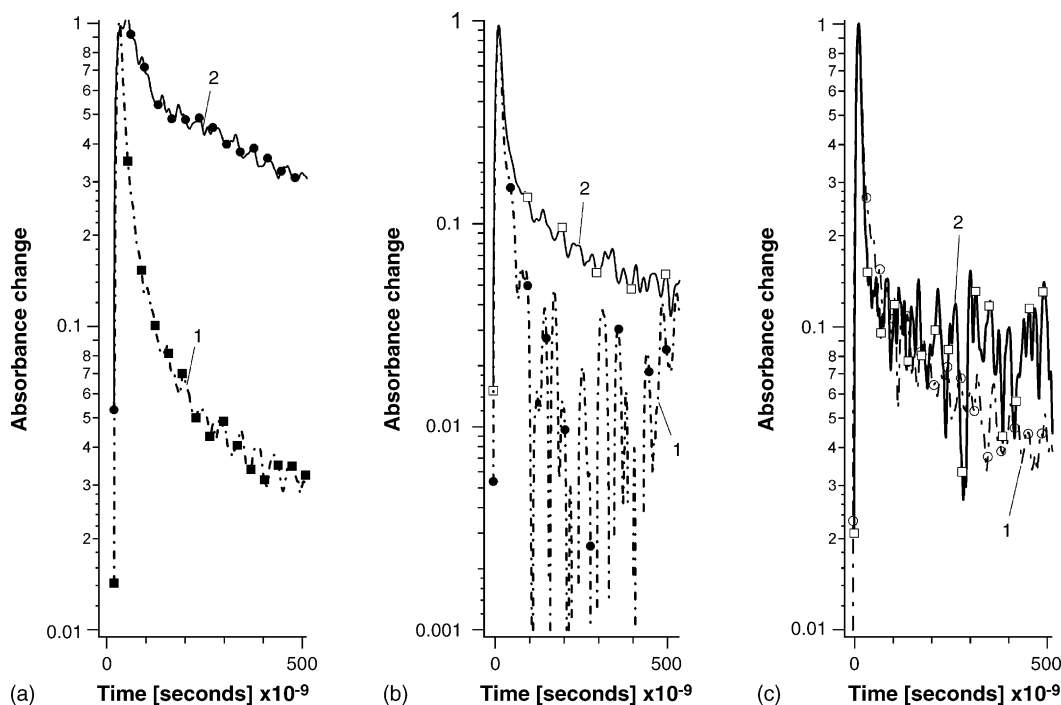


Fig. 7. Effect of the TiO<sub>2</sub> type used on the  $e^-$  decay in a colloid of TiO<sub>2</sub> in the absence and in the presence of  $3 \times 10^7$  CFU/ml *E. coli*. The  $e^-$  decay registered at  $\lambda = 820$  nm obtained from nanosecond laser photolysis laser photolysis: (a) Degussa P-25, (1) without *E. coli* ( $\tau = 70$  ns), (2) with *E. coli*, ( $\tau = 310$  ns); (b) S5-300B, (1) without *E. coli*, ( $\tau = 27$  ns), (2) with *E. coli* ( $\tau = 55$  ns); (c) S5-300A, (1) without *E. coli*, ( $\tau = 42$  ns), (2) with *E. coli*, ( $\tau = 56$  ns).

mediating *E. coli* inactivation for reasons not related directly to its BET area. *E. coli* is negatively charged in the pH region 3–9 [27], and the experiment has been carried out at a pH of 6 where TiO<sub>2</sub> is charged positively since we are in the region below the IEP = 7 (see Table 1). The surface charge seems not to play a significant role on the abatement rate of *E. coli* by S5-B-300 (IEP 4.9) and TKS 203 (IEP < 3) as shown in Fig. 6. The repulsion between the last two samples and *E. coli* at the pH of the photoreaction may be due to the *E. coli* cell wall membranes having negative carboxylic or acyl groups and positive amide or amine groups interacting on the cell wall in different topographical locations with the TiO<sub>2</sub> sample.

Fig. 7 shows the laser signals of the mixture of *E. coli* with TiO<sub>2</sub> Degussa P-25 with a neutral surface (see Table 1), with TiO<sub>2</sub> S5-A300 with acid surface anatase, S5-B300 with basic surface anatase. The signal was detected at 820 nm. From Fig. 7 it is readily seen that addition of *E. coli* affects the e<sup>-</sup> decay more meaningfully in the case of TiO<sub>2</sub> Degussa P-25 than in the case of TiO<sub>2</sub> S5-A300, and S5-B300. The ratios of mean rate constants of e<sup>-</sup> decay with and without *E. coli* addition are 4.4 for Degussa P-25, 2 for S5-300B, and 1.3 for S5-A300. In the case of TiO<sub>2</sub> Degussa P-25, h<sup>+</sup> is scavenged by *E. coli* more efficiently. At the same time under steady state illumination the TiO<sub>2</sub> Degussa P-25 was kinetically most efficient photocatalyst mediating the inactivation of *E. coli* within the first hour of reaction. A correlation between the efficiency of *E. coli* to scavenge h<sup>+</sup> at the TiO<sub>2</sub> surface and the kinetics of *E. coli* inactivation is possible when using these photocatalysts.

#### 4. Conclusions

This study investigated: (a) the interfacial charge transfer by induced laser photolysis between TiO<sub>2</sub> with cell wall membrane and *E. coli*, (b) the interaction of the charge carriers of selected TiO<sub>2</sub> colloids with different specific surface areas, surface charge and IEP on the cell wall components and *E. coli* and (c) the effect of ionic strength of the solution. In the nanosecond–millisecond time region, the wall cell membranes LPS, PE and the *E. coli* were observed to have a significant effect on the e<sup>-</sup> decay. The results obtained show that the h<sup>+</sup> scavenging by the cell wall is more effective than the scavenging of the photogenerated e<sup>-</sup>. The holes (h<sup>+</sup>) in TiO<sub>2</sub> have been shown to be scavenged by PE, LPS and *E. coli* leading to a decrease in e<sup>-</sup>/h<sup>+</sup> recombination rate. Salts like NaCl and CaCl<sub>2</sub> changed the rates of reaction of the cell wall membranes PE, LPS and *E. coli* with h<sup>+</sup>. They seem to regulate the binding between *E. coli* and the TiO<sub>2</sub> colloidal surface. The higher probability of h<sup>+</sup> scavenging by *E. coli* in TiO<sub>2</sub> Degussa P-25 detected by laser photolysis correlates with the higher inactivation rate of *E. coli* under the steady state illumination when using S5-A300 (acid surface anatase) and S5-B300 (basic surface anatase) for comparison purposes.

#### Acknowledgments

We thank the financial support of CTI/KTI TOP NANO 21 under Grant 5897.5 (Bern, Switzerland), COST D-19 under

Grant No. COO 2.0068, RFBR 03-03-32688, FASI 70504 (Moscow, Russia). We thank the help of P. Bowen and C. Morais of the Laboratory of Powder Technology, Department of Materials (EPFL) for their help with the electroacoustic measurements. We also thank the gifts of TiO<sub>2</sub> materials from (a) Degussa A.G., Obersdorf 11, Zoug, 6340 Baar, Switzerland, (b) Tayca samples of Mitsubishi Int. Corp., Kennedydamm 19, 40476, Dusseldorf, Germany, (c) Millennium Chemicals, 85 Avenue Victor Hugo, F-92563 Rueil Malmaison Cedex, France.

#### Appendix A. Supplementary data

Supplementary data associated with this article can be found, in the online version, at doi:10.1016/j.jphotochem.2005.12.028.

#### References

- [1] Y. Kikuchi, K. Sunada, T. Iyoda, K. Hashimoto, A. Fujishima, J. Photochem. Photobiol. A 106 (1997) 51.
- [2] K. Sunada, Y. Kikuchi, K. Hashimoto, A. Fujishima, Environ. Sci. Technol. 32 (1998) 726.
- [3] K. Sunada, T. Watanabe, K. Hashimoto, J. Photochem. Photobiol. A 156 (2003) 227, and references therein.
- [4] P. Maness, Sh. Smolinski, D. Blake, Z. Huang, E. Wolftrum, W. Jacoby, Appl. Environ. Microbiol. 65 (1999) 4094.
- [5] E. Wolftrum, J. Huang, D. Blake, P. Maness, Z. Huang, J. Fiest, W. Jacoby, Environ. Sci. Technol. 36 (2002) 3412.
- [6] C. Harper, A. Christensen, A. Egerton, P. Curtis, J. Gunlazuardi, J. Appl. Electrochem. 31 (2001) 623.
- [7] T. Matsunaga, T. Tomoda, T. Nakajima, H. Wake, FEMS Microbiol. Lett. 29 (1985) 211.
- [8] A. Mills, S. LeHunte, Photochem. Photobiol. A 108 (1997) 1.
- [9] A. Fujishima, T. Rao, D. Tryk, J. Photochem. Photobiol. C Rev. 1 (2000) 1.
- [10] B. Harm, Biological Effects of UV Radiation, Cambridge University Press, Cambridge, UK, 1993.
- [11] V. Nadochenko, A. Rincon, S. Stanka, J. Kiwi, J. Photochem. Photobiol. A 169 (2005) 131.
- [12] J. Kiwi, V. Nadochenko, J. Phys. Chem. B 108 (2004) 17675.
- [13] R. Bacsá, J. Kiwi, T. Ohno, P. Albers, V. Nadochenko, J. Phys. Chem. A 109 (2005) 5994.
- [14] M. Suwalsky, V. Schneider, H. Mansilla, J. Kiwi, J. Photochem. Photobiol. B 78 (2005) 253.
- [15] D. Adams, L. Brus, C. Chidsey, S. Creager, C. Creutz, Ch. Kagan, P. Kamat, M. Lieberman, S. Lindsay, R. Marcus, R. Metzger, M. Michel-Beyerle, J. Mille, M. Newton, D. Rolison, O. Sankey, K. Schanze, J. Yardley, X. Zhu, J. Phys. Chem. B 107 (2003) 6668.
- [16] G. Rincon, C. Pulgarin, Appl. Catal., B 49 (2004) 99.
- [17] G. Rincon, C. Pulgarin, Appl. Catal., B 51 (2004) 283.
- [18] G. Rincon, C. Pulgarin, Sol. Energy 77 (2004) 635.
- [19] J. Ireland, P. Klosterman, E. Rice, M. Clark, Appl. Environ. Microbiol. 59 (1993) 1668.
- [20] D. Blake, P. Maness, Z. Huang, Z. Wolftrum, J. Huang, Sep. Purif. Meth. 28 (1999) 1.
- [21] J. Kiwi, V. Nadochenko, Langmuir 21 (2005) 4631.
- [22] E.N. Uschakov, V. Nadochenko, S. Gromov, A. Vedernikov, N. Lobova, M. Alfimov, F. Gostev, A. Petrukhin, O. Sarkisov, Chem. Phys. 298 (2004) 251.
- [23] R.W. O'Brien, W.D. Cannon, N.W.J. Rowlands, Colloid Interface Sci. 173 (1995) 406.
- [24] J. Hunter, Colloids Surf. Sect. A 141 (1998) 37.
- [25] W. O'Brien, J. Fluid Mech. 190 (1988) 71.
- [26] J. Hunter, Colloids Surf. Sect. A 195 (2001) 205.
- [27] D.G. Parfitt, Progr. Surf. Membr. Sci. 11 (1976) 181.
- [28] P. Bowen, P.J. Dispersion, Sci. Technol. 23 (2002) 631.